

# A Search for Periodicity in the Light Curves of Selected Blazars

N. A. Kudryavtseva<sup>1,\*</sup> and T. B. Pyatunina<sup>†2</sup>

<sup>1</sup>*Astronomy Institute, St. Petersburg State University, St. Petersburg, Russia*

<sup>2</sup>*Institute of Applied Astronomy, St. Petersburg, Russia*

(Dated: 23rd September 2018)

We present an analysis of multifrequency light curves of the sources 2223 – 052 (3C 446), 2230 + 114 (CTA 102), and 2251 + 158 (3C 454.3), which had shown evidence of quasi-periodic activity. The analysis made use of data from the University of Michigan Radio Astronomy Observatory (USA) at 4.8, 8, and 14.5 GHz, as well as the Metsahovi Radio Astronomy Observatory (Finland) at 22 and 37 GHz. Application of two different methods (the discrete autocorrelation function and the method of Jurkevich) both revealed evidence for periodicity in the flux variations of these sources at essentially all frequencies. The periods derived for at least two of the sources – 2223 – 052 and 2251 + 158 – are in good agreement with the time interval between the appearance of successive VLBI components. The derived periods for 2251 + 158 ( $P = 12.4$  yr) and 2223 – 052 ( $P = 5.8$  yr) coincide with the periods found earlier by other authors based on optical light curves.

## 1. INTRODUCTION

Studies of the variability of active galactic nuclei (AGNs) represent an effective tool for investigating the nature of the activity and the mechanisms leading to its observable manifestations. The long-term variability of AGNs, including possible periodicity of the variations, has been studied and discussed in detail in a number of works [1–4]. Traditionally, a large fraction of studies dedicated to searches for periodicity have been based on optical observations, since the durations of the historical light curves in the optical are as long as  $\sim 100$  yr for some sources, while the maximum durations of radio light curves are no more than  $\sim 35$  yr. Although the results of such studies have often been contradictory,

---

\* [nadia@gong.astro.spbu.ru](mailto:nadia@gong.astro.spbu.ru)

the detection in 1995 of an optical flare in OJ 287 that had been predicted based on the period of 11.9 yr detected in the historical light curve provided convincing confirmation of the presence of periodic activity in this source [5]. Possible periodicity in the radio activity has also recently been detected for several objects [2, 3, 6]. It is interesting that the radio period found for AO 0235+164 coincides with the optical period [7]. This coincidence of the optical and radio periods testifies that the radiation in both wavebands has the same (synchrotron) nature, and arises in coincident or nearby regions. A similar conclusion was drawn in [8] based on a comparison of the properties of the polarized emission in the optical and in the radio at 43GHz.

As we indicated above, data on periodicity of the activity of AGNs are often contradictory or inconsistent. In some cases, different periods have been derived for a single object based on analyses of data for different time intervals, which could have both methodical and physical origins. From a methodical point of view, the lack of agreement between derived periods could be a consequence of the limited extent and irregularity of the observational series used, which leads to a period found using one section of the light curve differing from that found using a different section. In addition, the physical processes giving rise to quasi-periodic variations of the flux density can be divided into two types: primary processes that are associated with the periodic generation of perturbations at the "central engine" due to multiplicity of the central black hole, and secondary processes that arise during the propagation of perturbations along the jet, such as the propagation of shocks along the jet [9, 10] or recollimation [11] or precession of the jet [12]. It is obvious that secondary processes are more likely to be manifest on short time intervals, but, the longer the duration of a series of observations, the more likely it is that periodicity due to primary processes will appear. Quasi-periodic processes with various natures forming in various regions of the jet can also be superposed, complicating and confusing the pattern of the periodicity.

Currently, the most widely accepted hypothesis explaining both periodicity in the activity of AGNs and the activity itself is the presence of a multiple black hole at the galactic nucleus [13]. One drawback of this theory is the short lifetime of a system of black holes due to the loss of energy to gravitational radiation. This problem can be avoided if we consider the multiplicity of the black holes as a dynamical process, where the main black hole captures new companions on time scales that are comparable to the lifetime of the previous black-hole pair [14, 15].

As was shown in [16], in models with multiple black holes, the process leading to the appearance of the primary perturbations in the vicinity of the multiple black hole may not have a strictly periodic character. Therefore, we will think in terms of the presence of quasiperiods in the light curves of AGNs, rather than some strict periodic process. A good example is provided by OJ 287, which is the best observed and studied object in this context, and shows the presence of precisely quasiperiodic flux-density variations [15]. Nevertheless, the presence of such quasiperiodic behavior can be used to within known limits predict the epochs of flares, making it possible to verify multiple black-hole models, study the propagation of the associated perturbations along the jet in more detail, and plan future observations based on the expected activity phase of the source.

The monitoring of AGNs carried out at 4.8, 8, and 14.5 GHz at the University of Michigan Radio Astronomy Observatory (UMRAO, USA) [17] and at 22 and 37 GHz at the Metsahovi Radio Astronomy Observatory (MRAO, Finland) [18] over more than 30 yr present unique opportunities for studies of the long-term evolution of these objects. These databases have been analyzed earlier on the basis of structure functions [19, 20], wavelet analysis [2], and autocorrelation matrices [3], but the information that can be extracted for these data has not been exhausted.

In our earlier works [6, 21], based on an analysis of multifrequency light curves of selected blazars, we divided the observed radio flares into core events, which display low-frequency delays and are associated with primary perturbations in the core, and jet events, which appear simultaneously at all frequencies and are associated with the propagation of primary perturbations along the jet [10, 22]. We also defined the time intervals between successive core flares as the characteristic time scale for the development of activity in these blazars. The questions of how the characteristic time scale for the development of activity varies from source to source and whether these time scales are preserved over long times within a single source are of fundamental importance for our understanding of the nature of the activity. We present here estimates of possible periodic components in the light curves of several sources we have studied earlier, derived using the method of Jurkevich and the discrete autocorrelation function. The advantage of these methods is that they are independent of the form of the signal, and can be used to find periodicities not only when the signal is sinusoidal, as in the case of Fourier analysis.

## 2. LIGHT CURVES

We used the UMRAO and MRAO monitoring databases to carry out our searches for periodicity. Based on the results of our previous detailed analyses of flares in several blazars [6, 21], we selected three objects showing evidence for possible quasiperiodic flux variations. Table 1 presents a list of these objects, the observing frequencies  $\nu$  in GHz, the range of dates for which observations are available, the duration of the observational series in years  $\Delta T$ , and the number of flux measurements  $N$ . The durations of the observational series are very different for different objects and for different frequencies, and ranges from 17 to 38 yr.

## 3. METHOD FOR ANALYSIS OF THE LIGHT CURVES

### 3.1. Discrete Autocorrelation Function

The application of the discrete autocorrelation function [23] is designed to calculate the correlation coefficient between two series of irregularly distributed data as a function of the time shift between them. The method can also be used to search for periodicity if the two data series are identical. If there is a period in the light curve, the discrete autocorrelation function should exhibit a clear correlation at time shifts equal to zero and to the period. The closer the correlation coefficient is to unity, the more trustworthy is the identified period.

To determine the values of the discrete autocorrelation function for each pair of data  $(a_i, b_j)$ , we calculate the function *UDCF*:

$$UDCF_{ij} = \frac{(a_i - \bar{a})(b_j - \bar{b})}{\sqrt{\sigma_a^2 \sigma_b^2}},$$

where  $\bar{a}$ ,  $\bar{b}$  are the mean values of the data series and  $\sigma_a$ ,  $\sigma_b$  are the corresponding standard deviations. Each pair of data is associated with a time interval  $\Delta t_{ij} = t_j - t_i$ . The set of values  $UDCF_{ij}$  are divided into groups so that the time interval between the observation times  $\Delta t_{ij}$  falls into some interval around the trial time delay:  $\tau - \Delta\tau/2 \leq \Delta t_{ij} \leq \tau + \Delta\tau/2$ . Averaging the  $UDCF_{ij}$  values over each group yields the discrete autocorrelation function:

$$DCF(\tau) = \frac{1}{M} \sum UDCF_{ij}(\tau),$$

where  $M$  is the number of pairs in the group. The error is calculated using the formula

$$\sigma(\tau) = \frac{1}{M-1} \left\{ \sum [UDCF_{ij} - DCF(\tau)]^2 \right\}^{1/2}.$$

The discrete autocorrelation function often displays a flat peak. In such situations, we approximated this function with a Gaussian in order to more accurately estimate the period.

### 3.2. Method of Jurkevich

#### 3.2.1. Description of the method.

The method of Jurkevich [24] is based on analysis of the dispersions of the phase curves constructed for a series of trial periods. The essence of the method is that, the closer a trial period to the real period, the smaller the scatter of the points in the phase curve. To identify the period for which the dispersion reaches a minimum, phase curves are constructed for a series of trial periods, where the phase is defined by the relation

$$\varphi_i = \frac{T - T_0}{P} \pmod{1},$$

where  $P$  is the trial period and  $T_0$  is the time corresponding to the zero phase. The time  $T_0$  is usually taken to be the middle of the observational interval. Then, all the data are divided into  $m$  groups according to their phases, and the rms deviation is calculated for each group:

$$V_l^2 = \sum_{i=1}^{m_l} x_i^2 - m_l \bar{x}_l^2,$$

where  $m_l$  is the number of points in the group and  $\bar{x}_l$  is the mean value  $x_i$  for the group. Further, the sum of the mean square deviations over all groups is calculated:

$$V_m^2 = \sum_{i=1}^m V_l^2.$$

The appearance of a minimum in the function  $V_m^2$  at some trial period could indicate that this corresponds to a real period in the variations. Kidger et al. [25] proposed the use of a modified function  $V_m^2$  to estimate the trustworthiness of the identified periods:

$$f = \frac{1 - V_m^2}{V_m^2},$$

where here  $V_m^2$  is normalized to the value  $V_t^2$  calculated for the entire dataset. A value  $V_m^2 = 1$  corresponds to  $f = 0$ , and denotes an absence of periodicity in the data series. The values of periods can be found from a plot of the function  $f$ : values  $f \geq 0.5$  indicate very strong periodicity, while values  $f \leq 0.25$  indicate that, if any periodicity is present, it is manifest only very weakly. Another criterion for the trustworthiness of a period is the depth of the minimum of  $V_m^2$  relative to the noise. If this minimum is a factor of ten larger than the error in the "flat" part of the curve, the period corresponding to this minimum can be considered real [25]. We fit Gaussians to the plots of the modified function  $V_m^2$  in order to more accurately find the position of the minimum. We estimated the error in the resulting period formally as the half-width of the corresponding peak.

### 3.2.2. Search for false periods using Monte-Carlo simulations.

The irregularity of the observational series can lead to the appearance of false periods. We carried out Monte-Carlo simulations in order to separate out periods associated with real variability of the objects from those associated with the irregularity of the observations. The synthetic light curves generated in this way were analyzed using the method of Jurkevich. The artificial light curves were constructed from the real observations using the method presented in [4]: the observation times were retained, and the fluxes were chosen at random from the real light curve. Thus, any period found for these light curves can only be a consequence of the time distribution of the observations.

If periods detected in the synthetic data coincided with periods found for the real light curves, they were classified as false and were not considered further.

## 4. RESULTS OF THE ANALYSIS

### 4.1. 2223-052 (3C 446)

The source 2223 – 052 ( $z = 1.404$ ) is known to exhibit characteristics of a quasar or a BL Lac object, depend on its activity state. In its quiescent state, it displays strong emission lines characteristic of quasars, while a powerful continuum dominates in the active phase, giving rise to weak emission lines, as is characteristic for BL Lac objects [26]. Periods of

4.2 and 5.8 yr have been detected in the optical [26]; the period of 4.2 yr was subsequently confirmed in multiple studies [27, 28].

Figure 1 presents the light curves from 4.8 to 37 GHz. Flares of two types alternate in the light curve: narrow, single flares with inverted spectra (growing toward higher frequencies), and broad flares with nearly flat spectra. The time interval between a narrow flare and the following broad flare is about 6 yr, while the interval between two successive flares of the same type is about 12 yr. Applying the method of Jurkevich to the light curves of 2223 – 052 yielded with a high degree of confidence the presence of periods of  $5.8 \pm 0.5$  yr for all five frequencies, and  $9.8 \pm 0.5$  yr for all frequencies except 4.8 GHz (here and below, the presented periods are the average values over the various frequencies). Figure 3 presents the plot of the function  $V_m^2$  for the 8 GHz data, which illustrates the results. It is interesting that the detected period  $5.8 \pm 0.5$  yr coincides with the period of 5.8 yr found in [26] for the optical light curve of 2223 – 052. However, further observations in both the radio and optical are needed in order to confirm this agreement of the periods of 2223 – 052 in these two wavebands.

The discrete autocorrelation function yielded a period of  $10.9 \pm 0.2$  yr for 37, 22, and 14.5 GHz. Figure 2 presents the discrete autocorrelation function for 14.5 GHz. Table 2 gives a list of the derived periods, where  $\nu$  is the observing frequency in GHz,  $P_{Jurk}$  the period found using the method of Jurkevich (in years),  $f$  the confidence measure for  $P_{Jurk}$ ,  $P_{DACF}$  the period found using the discrete autocorrelation function (in years), and  $k$  the corresponding correlation coefficient.

Figure 1 presents light curves for 2223 – 052 for all the frequencies, with the flares corresponding to the period of  $5.8 \pm 0.5$  yr found with a high confidence level  $f$  using the method of Jurkevich indicated. We can see that this period describes the activity of the source well, i.e., the flares of 1984, 1990, 1996, and 2000. On the other hand, the discrete autocorrelation function detected only the 11-year period, possibly due to the coincidence in the structure of the "broad" and "narrow" flares when the light curve is shifted by 11 years. The question of both types of flares are associated with the birth of new superluminal components can be addressed using VLBI observations at 22 or 43 GHz .

The blazar 2223 – 052 was observed by Kellermann et al. [29] as part of a program of VLBI monitoring of AGNs at 15 GHz. These 15 GHz observations can provide information about large-scale processes in the evolution of the source and indicate the characteristic

time scale for activity cycles. Kellermann et al. [29] report the births of VLBI components at epochs  $1981.4 \pm 1.6$  and  $1994.0 \pm 0.8$ , marked on the light curve (Fig. 1) by vertical arrows. Given the possible uncertainties in determining the birth epochs of the components, these epochs are fairly close to the powerful flares of 1984 and 1996. A visual analysis of the maps obtained in the MOJAVE 15-GHz monitoring program [8], available on the MOJAVE website, suggest the birth of a new VLBI component in 2002. We can see from Fig. 1 that this component could be associated with the decay of a powerful flare in 2000. Taking into account the uncertainties in the birth epochs of VLBI components and the absence of VLBI observations before 1995, the births of observed components agree fairly well with the epochs of the powerful flares described by the period of  $5.8 \pm 0.5$  yr.

Note that only four six-year periods, and slightly more than two 11-year periods, are present in the light curve of 2223 – 052 (Table 1). Therefore, further observations at all frequencies are required in order to verify these periods. According to our estimates, the following flare should occur in 2007, and should be accompanied by the birth of a new component on VLBI scales. Taking into account the redshift of the source,  $z = 1.404$ , and applying the relation  $P = P_{obs}/(1 + z)$ , the detected periods in the rest frame of the source are 2.4 and 4.5 yr.

#### 4.2. 2230+114 (CTA 102)

2230 + 114 is a gamma-ray blazar at  $z = 1.037$  [30]. In 1965, Sholomitsky [31] published the first report of variability of this source, with a period of 102 days at 902 MHz. Although this result was not subsequently confirmed [32], variability was soon detected at shorter wavelengths [6].

Figure 4 presents the light curves of 2230 + 114 at all five frequencies. We can see that bright flares are observed approximately every eight years. The flares are characterized by the presence of fine structure on time scales appreciably shorter than one year. The amplitudes of the flares vary appreciably, but the positions of individual features in the flare structure are preserved [6]. It is interesting that not only the total amplitude of the flares in each eight-year cycle, but also the relative brightnesses in the fine-structure features, vary with time. In the first and third eight year cycles, the first subflare dominates, while the two first subflares have equal amplitudes in second cycle. All this gives rise to a complex



pattern for the variability, complicating a mathematical analysis.

The discrete autocorrelation function yielded periods of  $4.3 \pm 0.5$  yr at 14.5 GHz and  $8.4 \pm 0.1$  yr at 14.5 and 4.8 GHz (Table 3). Figure 5 presents the discrete autocorrelation function for 14.5 GHz. The method of Jurkevich yields periods of  $4.6 \pm 0.7$  yr at 37, 22, and 4.8 GHz and  $9.3 \pm 0.6$  yr at all frequencies except 8 GHz (Table 3, Fig. 6). Figure 7 presents the 14.5 GHz light curve with the intervals corresponding to the period  $4.3 \pm 0.5$  yr indicated. We can see that this period describes well both the powerful flares of 1981, 1990, and 1999 and the weaker flares 1986, 1995, and 2003, while the period  $8.4 \pm 0.1$  yr describes only the large-amplitude flares (1981, 1990, and 1999).

Jorstad et al. [33, 34] reported the birth of VLBI components in  $2230 + 114$  at epochs  $1994.28 \pm 0.02$ ,  $1995.19 \pm 0.04$ ,  $1996.08 \pm 0.02$ ,  $1997.9 \pm 0.2$ , and  $1999.54 \pm 0.04$  at 43GHz . Rantakyrö et al. [35] estimated the birth epochs and speeds of jet components based on all available VLBI observations in the literature. The birth epochs of the 43-GHz VLBI components are marked by arrows on the 37 GHz light curve (Fig. 8). Each birth epoch coincides with a flare at 37 GHz, but the irregular and insufficiently dense series of VLBI observations prevents a detailed comparison of the evolution of the light curve with the evolution of the VLBI source structure. The detailed light-curve analysis of Pyatunina et al. [6, 21] showed the presence of activity cycles with a characteristic variability time scale of  $8.04 \pm 0.3$  yr, in good agreement with the period we have found here,  $8.4 \pm 0.1$  yr.

The available light curve encompasses about six four-year and three eight-year periods (Table 1), and further observations are required to verify these periods. According to our estimates, the following flare should occur in 2007. Taking into account the source redshift, the derived periods in the rest frame of the source are 2.1 and 4.1 yr.

#### 4.3. *2251+158 (3C 454.3)*

$2251 + 158$  is a gamma-ray blazar with a redshift of  $z = 0.859$  [30]. By identifying the main components of the autocorrelation matrix using a neural network, Ciaramella et al. [3] found the period 6.07–6.55 yr for this object at 4.8, 8, 14.5, 22, and 37 GHz. Cheng-yue [36] found a period of 12.39 yr in the optical based on a hundred-year historical light curve in the *B* band.

The light curve of  $2251+158$  is presented in Fig. 9. We can see that powerful flares

are observed approximately every 12 years. Our analysis using the discrete autocorrelation function detected two periods at all five frequencies:  $6.2 \pm 0.1$  and  $12.4 \pm 0.6$  yr (Table 4). As an example, Fig. 10 presents the discrete autocorrelation function for the 4.8 GHz light curve. The method of Jurkevich detected the periods  $6.1 \pm 0.6$  and  $11.9 \pm 1.1$  yr with high confidence at all frequencies (Table 4); this is clearly visible in Fig. 11, which shows a plot of the function  $V_m^2$  for the 4.8-GHz light curve.

Thus, the periods  $6.2 \pm 0.1$  and  $12.4 \pm 0.6$  yr were detected at all five frequencies by both the method of Jurkevich and the discrete autocorrelation function. The light curves of 2251+158 encompass up to six six-year periods, while only three 12-year periods are included in the most extensive light curve at 8 GHz; further observations are required to verify the presence of the latter period (Table 1). The period  $6.2 \pm 0.1$  yr is in good agreement with the periods reported earlier [3]. Figure 9 presents the light curve of 2251 + 158 with the positions of the flares corresponding to the 6.2 and 12.4-year periods marked. The  $12.4 \pm 0.6$ -year period is determined by the flares of 1967, 1982, and 1995, while the  $6.2 \pm 0.1$ -year period is determined by these flares, together with the somewhat weaker intermediate flares of 1975 and 1987.

The quasar 2251 + 158 is one of the best observed radio sources, and a large amount of information about its VLBI structure has been published, making it possible to compare variations in the source structure with variations in the light curves. Pauliny-Toth [37, 38] reported the births of components at epochs 1966 and  $1981.7 \pm 0.8$  at 2.8 cm. Cawthorne and Gabuzda [39] reported the probable birth of a component at epoch 1988.2 based on polarization observations at 5 GHz. Based on their monitoring of gamma-ray blazars at 43GHz, Jorstad et al. [33] derived the birth epochs for there VLBI components  $1994.45 \pm 0.03$  (B1),  $1995.05 \pm 0.05$  (B2), and  $1995.59 \pm 0.14$  (B3). The 43-GHz observations of Gomez et al. [40] and Kembal et al. [41] indicate the possible appearance of components at epochs 1995.7 and 1994.9, in agreement with the results of Jorstad et al. [33]. The arrows in Fig. 9 mark the published birth epochs for VLBI components. We can see that these birth epochs are in good agreement with the epochs of powerful flares, allowing for the fact that there were no regular VLBI observations of 2251 + 158 before 1981. The presence of several components during the flare of 1995 can be explained by the good spatial resolution provided at 43GHz compared to the observations at lower frequencies. Thus, based on the available data on the birth epochs of VLBI components, the time interval between the generation of new

components is about 6.3yr , in good agreement with the six-year period we have found for the radio light curves. The analysis of the frequency delays and spectral evolution of flares carried out by Pyatunina et al. [21] showed the presence of a characteristic variability time scale of about 13yr , in agreement with the detected period of  $12.4 \pm 0.6$  yr.

Thus, the periods of  $6.2 \pm 0.1$  and  $12.4 \pm 0.6$  yr found formally using the period-search methods are in good agreement with the characteristic time scale for variations in the VLBI structure, as well as the frequency delays and spectra of flares. According to our estimates, the next flare in 2251 + 158 should occur in 2007, have an amplitude comparable to the flare of 1995, and be accompanied by the appearance of a new VLBI component. Taking into account the source redshift,  $z = 0.859$ , the detected periods in the source rest frame are 3.3 and 6.7 yr.

Note also that our detected period  $12.4 \pm 0.6$  yr coincides with the period of 12.39 yr found by Cheng-yue [36] for the hundred-year historical optical light curve in the  $B$  band. The agreement of the periods found in the optical and radio for  $AO\ 0235+164$  [7] and  $BL\ Lac$  [42] may indicate that the same radiation mechanism is responsible for the variability in these two wavebands. Correlations between the optical and radio emission of 2251 + 158 have been reported by a number of authors: Pomphrey et al. [43] found a strict correlation with a time delay of 1.2 yr, Balonek [44] reported possible correlations with delays of 180, 285, and 310 days, and Tornikoski et al. [45] and Hanski et al. [46] identified simultaneous events in the optical and radio. The presence of a strict correlation suggests a strict coincidence of the periods in the two wavebands, but, given the length of the period, its confirmation requires further observations in both the optical and radio.

## 5. CONCLUSION

Our analysis of the light curves of 2223 – 052, 2230 + 114, and 2251 + 158 at 4.8, 8, 14.5, 22, and 37 GHz based on the UMRAO (USA) and MRAO (Finland) monitoring data has confirmed the presence of periodicity in the flux variations of these sources. The flux variations in 2223 – 052 occur on characteristic time scales of  $5.8 \pm 0.5$  and  $10.9 \pm 0.2$  yr, with the six-year period being in good agreement with the time scale for the appearance of VLBI components at 15 GHz. In addition, the detected period of 5.8 yr coincides with the period found earlier for the optical light curve (5.8 yr) [26]. The light curves for 2230 + 114 show

characteristic variation time scales of  $4.3 \pm 0.5$  and  $8.4 \pm 0.1$  yr, but a comparison with the evolution of the VLBI structure of this source is complicated by the absence of observations during the early part of the radio light curves. Periods of  $6.2 \pm 0.1$  and  $12.4 \pm 0.6$  yr were detected in the light curves of 2251 + 158, and a comparison with published VLBI data shows that the 6.2-year period is in good agreement with the time scale for the evolution of the VLBI structure. The radio period of  $12.4 \pm 0.6$  yr also agrees with the period derived by Cheng-yue [36] based on a hundred-year historical optical light curve.

## 6. ACKNOWLEDGMENTS

This work has made use of the monitoring data of the University of Michigan Radio Astronomy Observatory. The authors thank Hugh and Margo Aller for presenting us with these data, as well as for our long-standing fruitful collaboration. This work has also made use of monitoring data from the Metsahovi Radio Astronomy Observatory. We thank Harri Terasranta for fruitful collaboration and providing us with these data. The work was supported by a grant from the Ministry of Education of the Russian Federation (grant no. 37840). N.A. Kudryavtseva thanks the President of the Russian Federation for financial support in 2004–2005.

- 
1. M. F. Aller, H. D. Aller and P. A. Hughes, *Astrophys. J.*, **586**, 33 (2003).arXiv:astro-ph/0211265
  2. B. C. Kelly, P. A. Hughes, H. D. Aller and M. F. Aller, *Astrophys. J.*, **591**, 695 (2003).arXiv:astro-ph/0301002
  3. A. Ciaramella, C. Bongardo, H. D. Aller, M. F. Aller, *et al.*, *Astron. Astrophys.*, **419**, 485 (2004).arXiv:astro-ph/0401501
  4. J. H. Fan, R. G. Lin, G. Z. Xie, *et al.*, *Astron. Astrophys.*, **381**, 1 (2002).
  5. T. Pursimo, L. O. Takalo, A. Sillanpää, *et al.*, *Astron. Astrophys. Suppl. Ser.*, **146**, 141 (2000).
  6. T. B. Pyatunina, N. A. Kudryavtseva, D. C. Gabuzda, *et al.*, in "Future Directions in High Resolution Astronomy: A Celebration of the 10th Anniversary of the VLBA", *Astron. Soc. Pac. Conf. Ser.*, **340**, 113; arXiv:astro-ph/0502171 (2005).
  7. (C. M. Raiteri, M. Villata, H. D. Aller, M. F. Aller, *et al.*, *Astron. Astrophys.*, **377**, 396 (2001).arXiv:astro-ph/0108165
  8. M. L. Lister, in "Future Directions in High Resolution Astronomy: A Celebration of the 10th Anniversary of the VLBA", *Astron. Soc. Pac. Conf. Ser.*, **340** (2005) (in press).
  9. J. L. Gomez, J. M. A. Marti, *at al.*, *Astrophys. J. Lett.*, **482**, 33 (1997).
  10. T. B. Pyatunina, S. G. Marchenko, *et al.*, *Astron. Astrophys.*, **358**, 451 (2000).
  11. J. L. Gomez, in "Future Directions in High Resolution Astronomy: A Celebration of the 10th Anniversary of the VLBA", *Astron. Soc. Pac. Conf. Ser.*, **340** (2005) (in press).arXiv:astro-ph/0501013
  12. A. M. Stirling, T. V. Cawthorne, J. A. Stevens, *et al.*, *MNRAS*, **341**, 405 (2003).
  13. A. P. Lobanov, J. Roland, in "6th European VLBI Network Symposium on New Developments in VLBI Science and Technology", ed. by E. Ros, R. W. Porcas et al. (Max-Planck-Institut fuer Radioastronomie, Bonn), 121 (2002).
  14. M. G. Haehnelt, IAU Symp. 159, "Multi-Wavelength Continuum Emission of AGN", ed. T. J.-L. Courvoisier, A. Blecha (Dordrecht: Kluwer), 279 (1994).
  15. M. R. Kidger, *Astron. J.*, **119**, 2053 (2000).
  16. B. Sundelius, M. Wahde, H. J. Lehto, M. J. Valtonen, *Astrophys. J.*, **484**, 180S (1997).
  17. H. D. Aller, M. F. Aller, *Bull. Am. Astron. Soc.*, **28**, 1406 (1996).
  18. H. Teräsraanta, M. Tornikoski, A. Mujunen, *et al.*, *Astron. Astrophys. Suppl. Ser.*, **132**, 305

- (1998).
19. P. A. Hughes, H. D. Aller, M. F. Aller, *Astrophys. J.*, **396**, 469 (1992).
  20. M. Lainela, E. Valtaoja, *Astrophys. J.*, **416**, 485 (1993).
  21. T. B. Pyatunina, N. A. Kudryavtseva, D. C. Gabuzda, *et al.*, in Proc. of the All-Russia Astronomical Conference "Horizons of the Universe", Moscow, p.109 (2004).
  22. J. F. Zhou, X. Y. Hong, D. R. Jiang, T. Venturi, *Astrophys. J.*, **540**, L13 (2000).arXiv:astro-ph/0009452
  23. R. A. Edelson, J. H. Krolik, *Astrophys. J.*, **333**, 646E (1988).
  24. I. Jurkevich, *Astrophys. Space Sci.*, **13**, 154 (1971).
  25. M. R. Kidger, L. Takalo, A. Sillanpää, *Astron. Astrophys.*, **264**, 32 (1992).
  26. C. Barbieri, S. Cristiani, S. Omizzolo, G. Romano, *Astron. Astrophys.*, **142**, 316 (1985).
  27. J. R. Webb, A. G. Smith, *et al.*, *Astron. J.*, **95**, 374 (1988).
  28. C. Barbieri, R. Vio, E. Cappellaro, M. Turatto, *Astrophys. J.*, **359**, 63 (1990).
  29. K. I. Kellermann, M. L. Lister, D. C. Homan, *et al.*, *Astrophys. J.*, **609**, 539 (2004).arXiv:astro-ph/0403320
  30. J. J. Blom, H. Bloemen, K. Bennett, *et al.*, *Astron. Astrophys.*, **295**, 330 (1995).
  31. G. B. Sholomitsky, *IBVS*, **83**, 1S (1965).
  32. Y. Terzian, *Astron. J.*, **71**, 1030 (1966).
  33. S. G. Jorstad, A. P. Marscher, *et al.*, *Astrophys. J. Suppl. Ser.*, **134**, 181 (2001).arXiv:astro-ph/0101570
  34. S. G. Jorstad, A. P. Marscher, *et al.*, *Astron. J.* (2005)(in press); arXiv:astro-ph/0502501.
  35. F. T. Rantakyrö, K. Wiik, M. Tornikoski, *et al.*, *Astron. Astrophys.*, **405**, 473 (2003).
  36. Cheng-yue Su, *Chinese Astronom. Astrophys.*, **25**, 153 (2001).
  37. I. I. K. Pauliny-Toth, R. W. Porcas, J. A. Zensus, *et al.*, *Nature*, **328**, 778 (1987).
  38. I. I. K. Pauliny-Toth, in IAU Colloq. 164, "Radio Emission from Galactic and Extragalactic Compact Sources", ed. J. A. Zensus et al., 25 (1998).
  39. T. V. Cawthorne and D. C. Gabuzda, *MNRAS*, **278**, 861 (1996).
  40. J. L. Gomez, A. P. Marscher, A. Alberdi, *Astrophys. J.*, **522**, 74 (1999).arXiv:astro-ph/9905206
  41. A. J. Kemball, P. J. Diamond, I. I. K. Pauliny-Toth, *Astrophys. J.*, **464**, L55 (1996).
  42. M. Villata, C. M. Raiteri, H. D. Aller, *et al.*, *Astron. Astrophys.*, **424**, 497 (2004).
  43. R. B. Pumphrey, A. G. Smith, R. J. Leacock, *et al.*, *Astron. J.*, **81**, 489 (1976).

44. T. J. Balonek, Ph.D. Thesis, University of Massachusetts (1982).
45. M. Tornikoski, E. Valtaoja, H. Teräsraanta, *et al.*, *Astron. Astrophys.*, **289**, 673 (1994).
46. M. T. Hanski, L. O. Takalo, E. Valtaoja, *Astron. Astrophys.*, **394**, 17 (2002).

*Translated by D. Gabuzda*

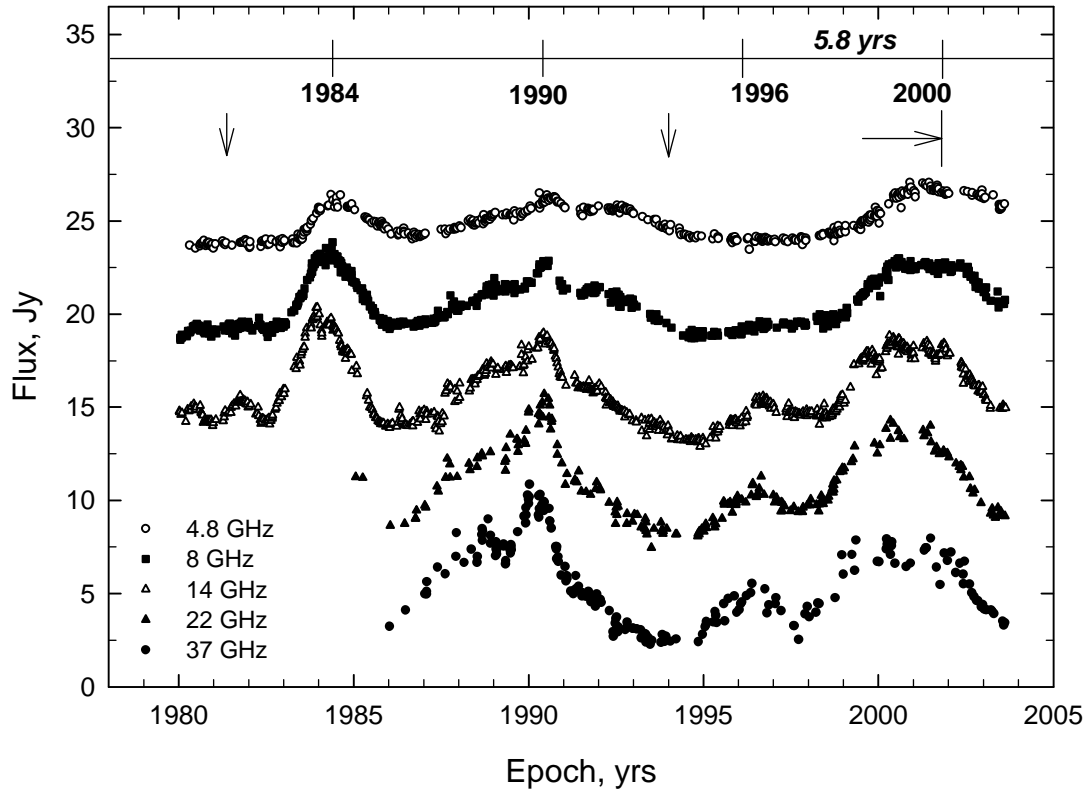


**Figure 1.** Light curves of 2223-052 for 37, 22, 14.5, 8, and 4.8 GHz. For ease of viewing, the curves have been shifted relative to each other by 5 Jy. The arrows mark the birth epochs of VLBI components.



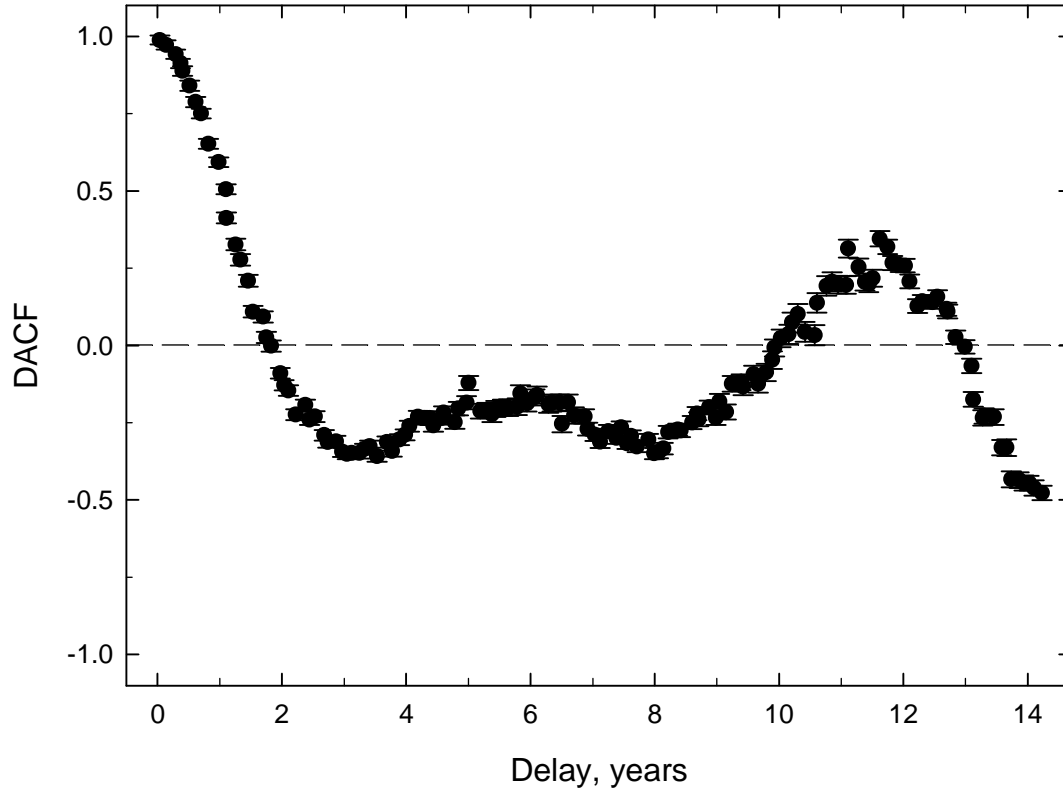


**Figure 2.** Plot of the discrete autocorrelation function constructed for 2223-052 at 14.5 GHz.

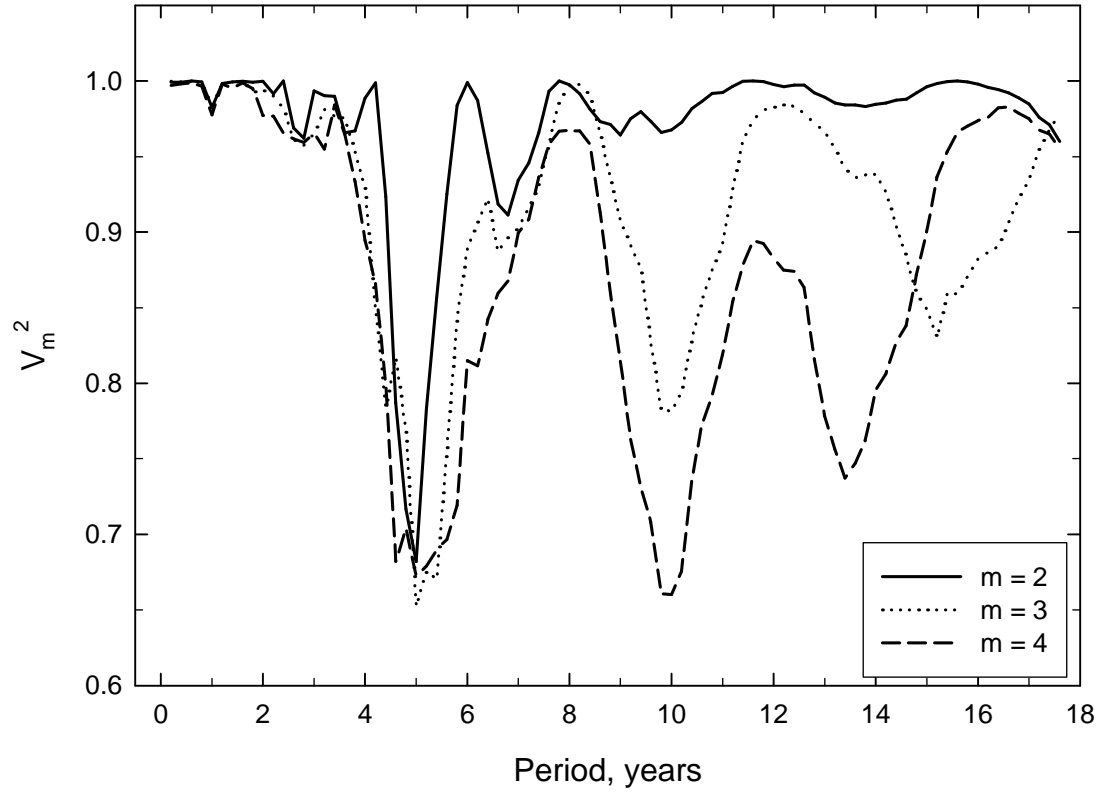


**Figure 3.** Results of the period search for 2223-052 at 8 GHz using the method of Jurkevich. Plots for various bin numbers for the phase curve are presented.

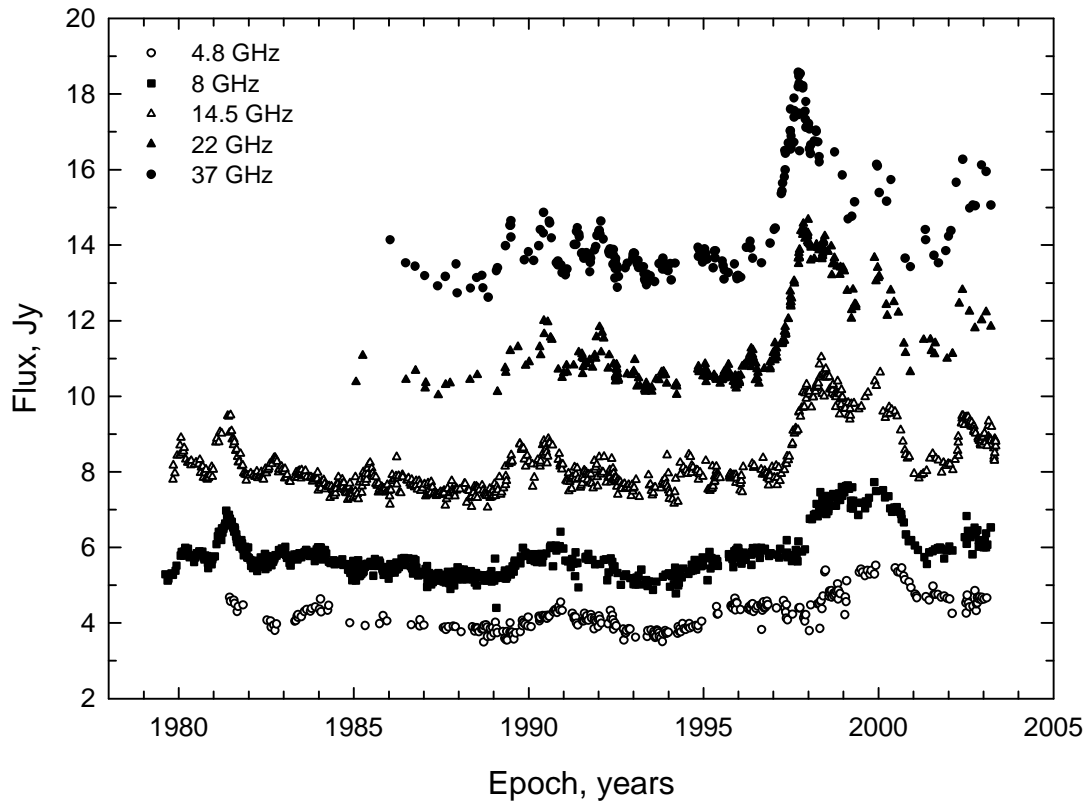


**Figure 4.** Light curves of 2230+114 for 37, 22, 14.5, 8, and 4.8 GHz. For ease of viewing, the curves have been shifted relative to each other in flux.

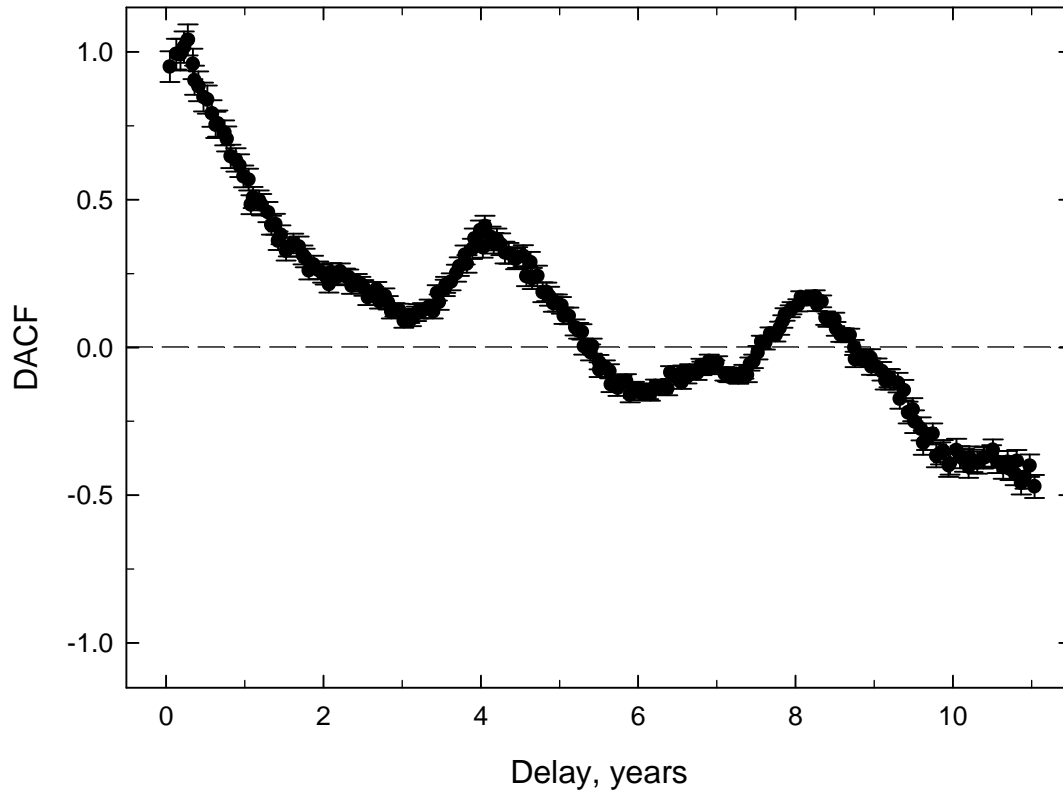
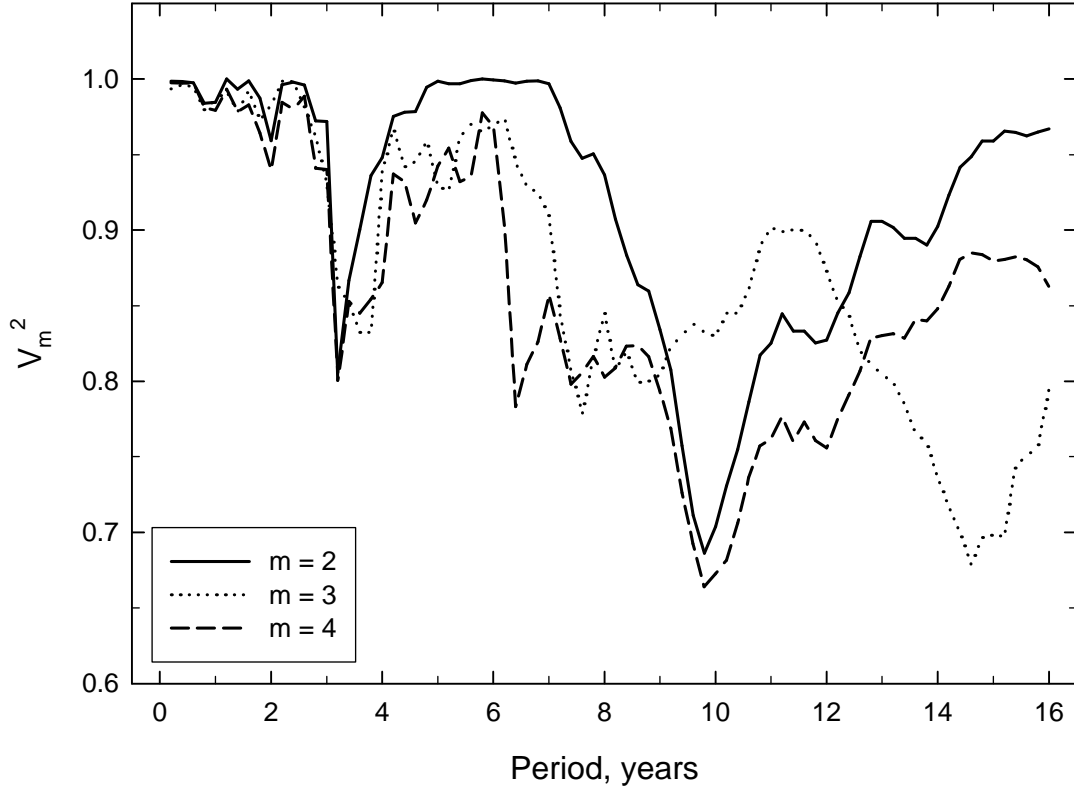
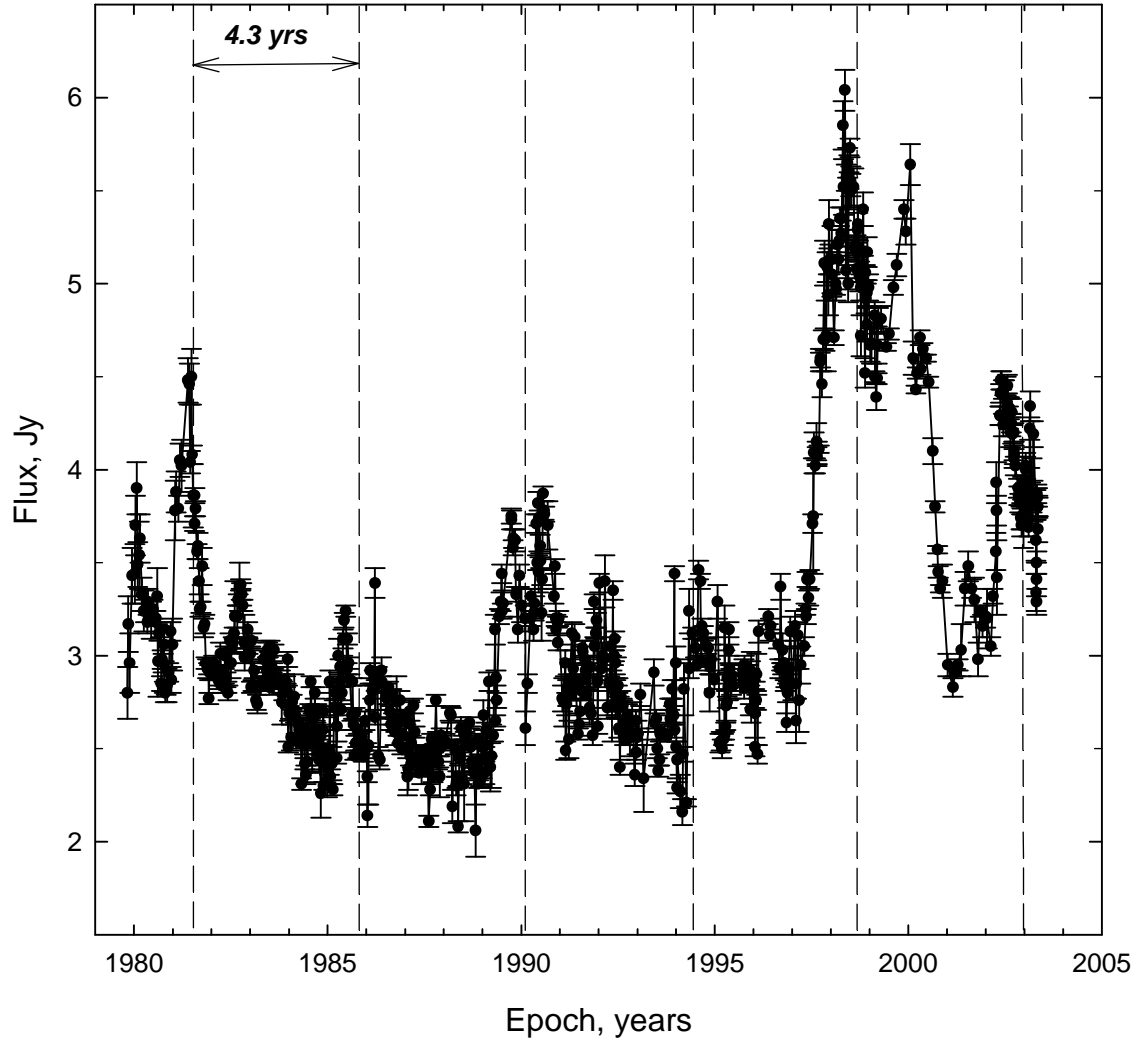


Figure 5. Discrete autocorrelation function for 2230+114 at 14.5 GHz.



**Figure 6.** Results of the period search for 2230+114 at 4.8 GHz using the method of Jurkevich. Plots for various bin numbers for the phase curve are presented.



**Figure 7.** Light curve of 2230+114 at 14.5 ± 6. The dotted lines mark intervals corresponding to the 4.3 ± 0.5-year period.

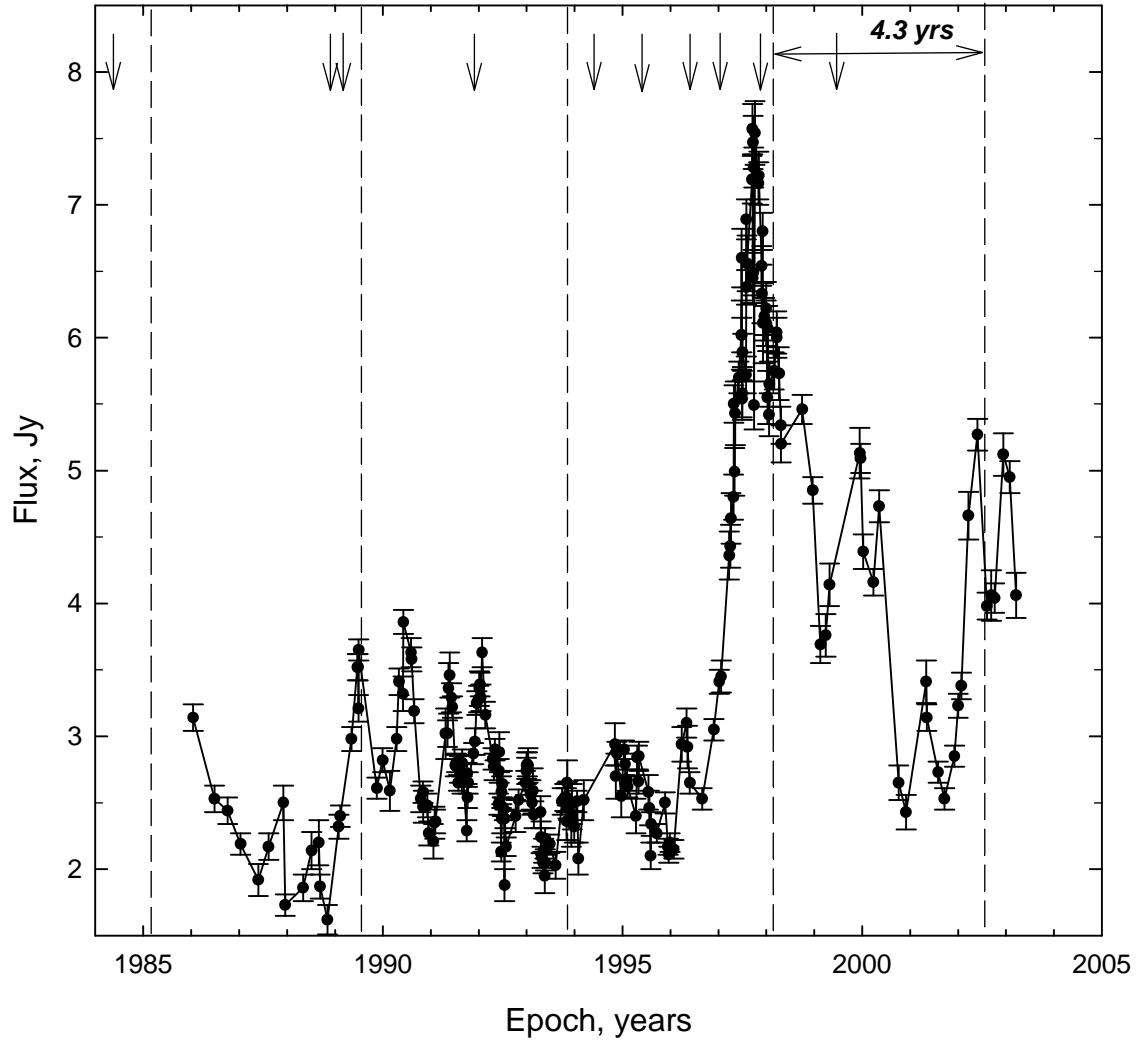


**Figure 8.** Light curve of 2230+114 at 37 GHz. The dotted lines mark intervals corresponding to the  $4.3 \pm 0.5$ -year period. The arrows mark the birth epochs of VLBI components at 43GHz [33–35].

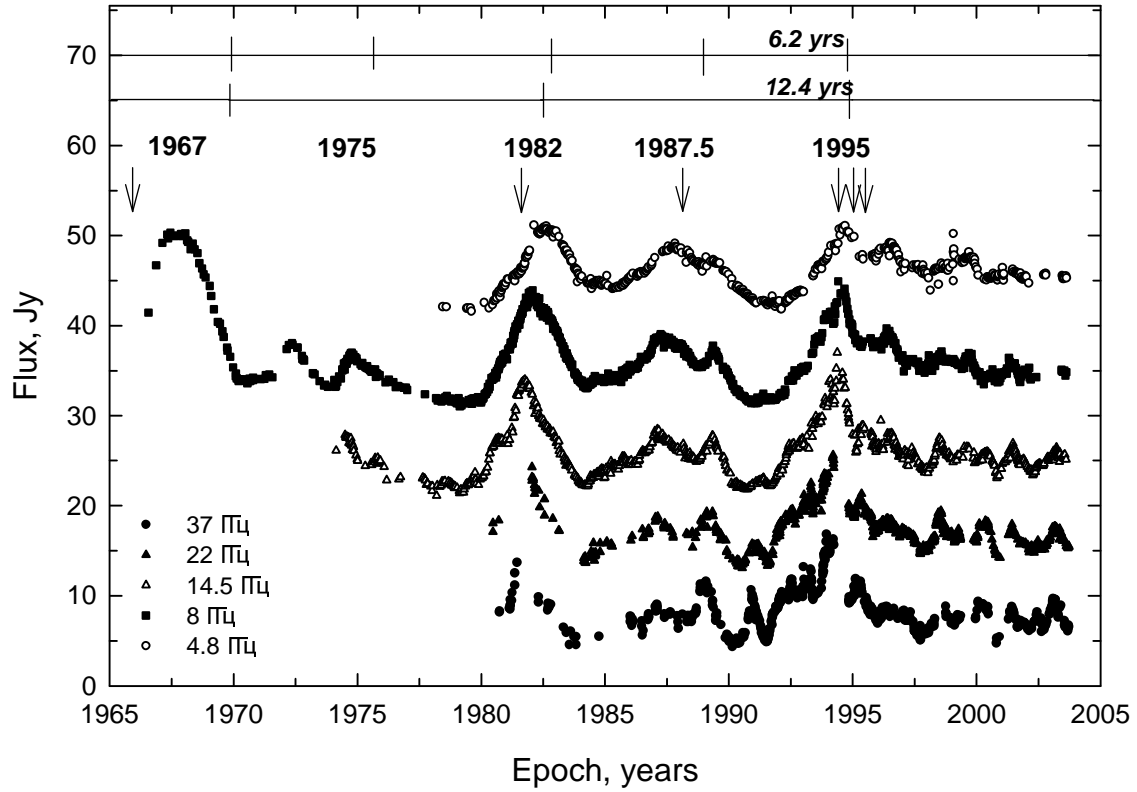


**Figure 9.** Light curves for 2251+158 at 37, 22, 14.5, 8, and 4.8 GHz. For ease of viewing, the curves have been shifted relative to each other by 8 Jy. The arrows mark the birth epochs of VLBI components.



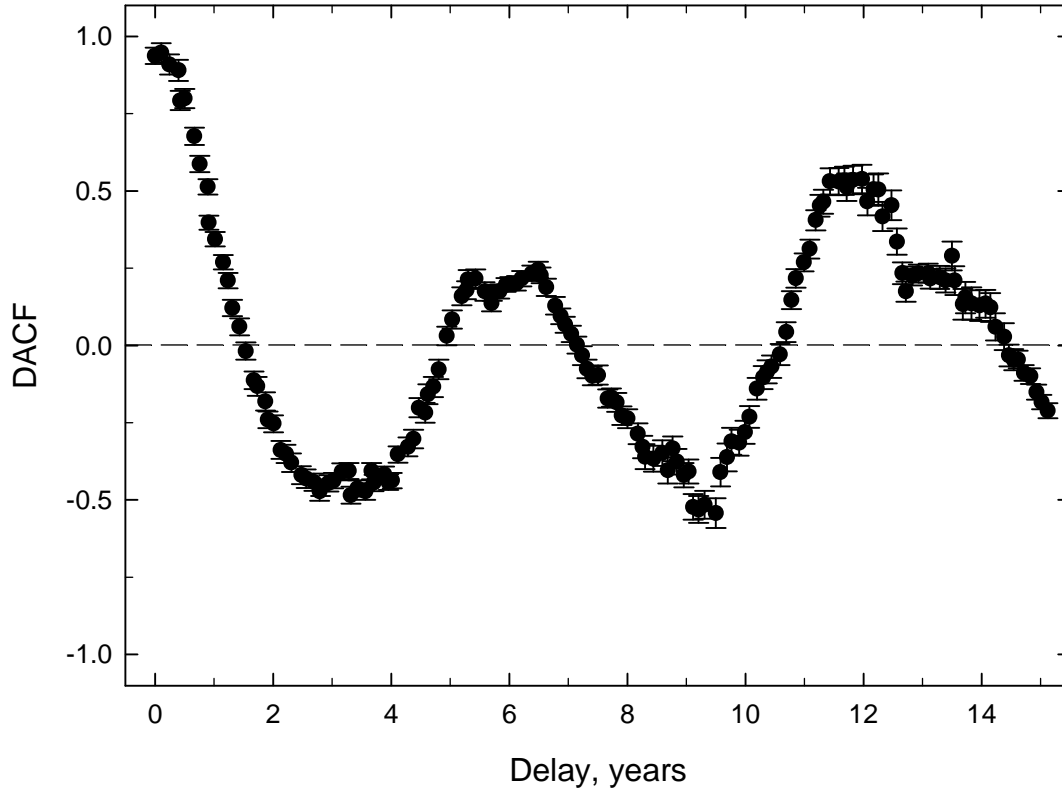
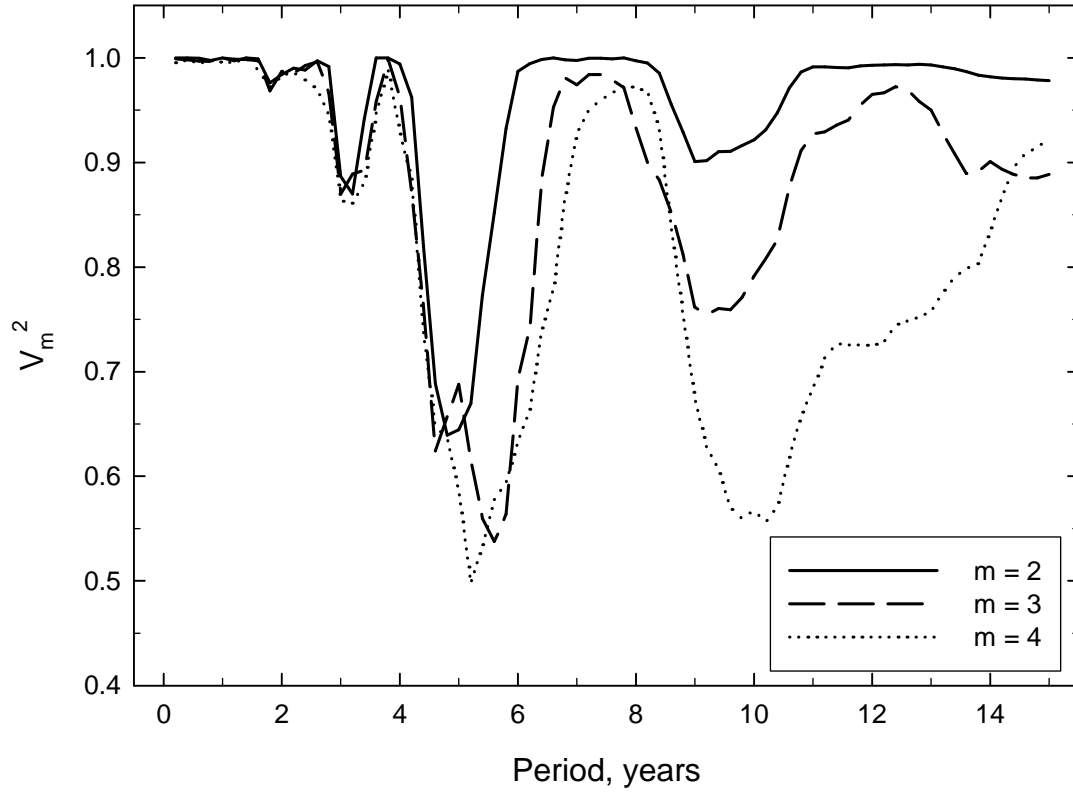


Figure 10. Discrete autocorrelation function for 2251+158 at 4.8 GHz.



**Figure 11.** Results of the period search for 2251+158 at 4.8 GHz using the method of Jurkevich. Plots for various bin numbers for the phase curve are presented.

**Table 1.** List of objects and characteristics of the light curves

Object	$\nu$ , (GHz)	Interval of observations	$\Delta T$ , yr	N
2223-052 (3C 446)	37	1986.0 - 2003.6	17.6	212
	22	1985.0 - 2003.6	18.6	220
	14.5	1980.0 - 2003.6	23.6	790
	8	1980.0 - 2003.6	23.6	735
	4.8	1980.3 - 2003.6	23.3	520
2230+114 (CTA 102)	37	1986.0 - 2003.2	17.2	217
	22	1985.1 - 2003.2	18.1	288
	14.5	1979.8 - 2003.3	23.5	725
	8	1974.6 - 2003.2	28.6	687
	4.8	1981.5 - 2003.1	21.6	314
2251+158 (3C 454.3)	37	1980.7 - 2003.7	23.0	623
	22	1980.5 - 2003.7	19.5	749
	14.5	1974.1 - 2003.6	29.5	925
	8	1966.6 - 2003.6	37.0	1026
	4.8	1978.4 - 2003.6	25.2	565

**Table 2.** Detected periods for 2223-052 (3T 446)

$\nu$ (GHz)	$P_{Jurk, yr}$	f	$P_{DACF, yr}$	k
37	$4.2 \pm 0.4$	0.26		
	$8.9 \pm 2.5$	2.55	$10.7 \pm 2.5$	0.85
22	$6.9 \pm 2.2$	1.83		
	$11.1 \pm 2.4$	2.55	$10.6 \pm 1.6$	0.85
14.5	$5.6 \pm 1.3$	0.52		
	$9.5 \pm 0.7$	1.21	$11.3 \pm 3.3$	0.25
8	$5.3 \pm 1.1$	0.56	—	—
	$9.9 \pm 1.1$	0.54		
4.8	$7.2 \pm 0.7$	0.39	—	—

**Table 3.** Detected periods for 2230+114 (CTA 102)

$\nu$ (GHz)	$P_{Jurk, yr}$	f	$P_{DACF, yr}$	k
37	$5.2 \pm 0.7$	0.60	—	—
	$9.7 \pm 1.5$	0.62		
22	$4.9 \pm 0.4$	0.60	—	—
	$8.4 \pm 2.3$	0.47		
14.5			$4.3 \pm 0.5$	0.41
	$9.2 \pm 2.0$	0.22	$8.3 \pm 1.2$	0.17
4.8	$3.8 \pm 0.8$	0.28		
	$9.8 \pm 2.1$	0.46	$8.5 \pm 1.2$	0.10

**Table 4.** Detected periods for 2251+158 (3C 454.3)

$\nu$ (GHz)	$P_{Jurk, yr}$	f	$P_{DACF, yr}$	k
37	$5.7 \pm 1.8$	0.88	$6.2 \pm 1.4$	0.24
	$11.6 \pm 2.8$	1.0	$12.6 \pm 1.4$	0.26
22	$6.7 \pm 0.9$	0.35	$6.3 \pm 1.9$	0.14
	$12.1 \pm 0.9$	0.47	$12.6 \pm 2.4$	0.52
14.5	$5.7 \pm 1.0$	0.86	$6.2 \pm 2.5$	0.24
	$10.5 \pm 0.9$	0.45	$12.5 \pm 1.6$	0.63
8	$6.7 \pm 0.8$	0.19	$6.1 \pm 3.5$	0.15
	$13.5 \pm 1.2$	0.44	$13.4 \pm 1.8$	0.45
4.8	$5.5 \pm 1.1$	0.86	$6.1 \pm 1.4$	0.24
	$11.7 \pm 2.6$	0.95	$11.8 \pm 1.2$	0.55